Impact of amyloid and tau positivity on longitudinal brain atrophy in cognitively normal individuals

Motonobu Fujishima[1]* , Yohei Kawasaki[2,3] , Toshiharu Mitsuhashi[4] , Hiroshi Matsuda[5,6] and for the Alzheimer's Disease Neuroimaging Initiative

Abstract

Background Individuals on the preclinical Alzheimer's continuum, particularly those with both amyloid and tau positivity (A+T+), display a rapid cognitive decline and elevated disease progression risk. However, limited studies exist on brain atrophy trajectories within this continuum over extended periods.

Methods This study involved 367 ADNI participants grouped based on combinations of amyloid and tau statuses determined through cerebrospinal fluid tests. Using longitudinal MRI scans, brain atrophy was determined according to the whole brain, lateral ventricle, and hippocampal volumes and cortical thickness in AD-signature regions. Cognitive performance was evaluated with the Preclinical Alzheimer's Cognitive Composite (PACC). A generalized linear mixed-effects model was used to examine group×time interactions for these measures. In addition, progression risks to mild cognitive impairment (MCI) or dementia were compared among the groups using Cox proportional hazards models.

Results A total of 367 participants (48 A+T+, 86 A+T−, 63 A−T+, and 170 A−T−; mean age 73.8 years, mean follow-up 5.1 years, and 47.4% men) were included. For the lateral ventricle and PACC score, the A+T− and A+T+ groups demonstrated statistically significantly greater volume expansion and cognitive decline over time than the A−T− group (lateral ventricle: β=0.757 cm^3/year [95% confidence interval 0.463 to 1.050], $P<.001$ for A+T−, and β=0.889 cm^3/year [0.523 to 1.255], $P<.001$ for A+T+; PACC: β=−0.19 /year [−0.36 to −0.02], $P=.029$ for A+T−, and β=−0.59 /year [−0.80 to −0.37], $P<.001$ for A+T+). Notably, the A+T+ group exhibited additional brain atrophy including the whole brain (β=−2.782 cm^3/year [−4.060 to −1.504], $P<.001$), hippocampus (β=−0.057 cm^3/year [−0.085 to −0.029], $P<.001$), and AD-signature regions (β=−0.02 mm/year [−0.03 to −0.01], $P<.001$). Cox proportional hazards models suggested an increased risk of progressing to MCI or dementia in the A+T+ group versus the A−T− group (adjusted hazard ratio=3.35 [1.76 to 6.39]).

Conclusions In cognitively normal individuals, A+T+ compounds brain atrophy and cognitive deterioration, amplifying the likelihood of disease progression. Therapeutic interventions targeting A+T+ individuals could be pivotal in curbing brain atrophy, cognitive decline, and disease progression.

Keywords Preclinical, Alzheimer's disease, Longitudinal MRI, Tau, Amyloid-β

*Correspondence:
Motonobu Fujishima
fujishima-nii@umin.ac.jp
Full list of author information is available at the end of the article

Fujishima *et al. Alzheimer's Research & Therapy* (2024) 16:77

Page 2 of 16

Background

From 2022–2023, the results of phase III clinical trials of the anti-amyloid-beta (Aβ) monoclonal antibodies lecanemab and donanemab for Alzheimer's disease (AD) were published [1, 2], with the former approved by the U.S. Food and Drug Administration (FDA) and the latter under review for approval. These disease-modifying drugs were designed based on the amyloid cascade hypothesis in AD [3]. The hypothesis is that Aβ aggregates and forms fibrils outside of neurons in the cerebral cortex; then, hyperphosphorylated tau aggregates and forms neurofibrillary tangles within neurons, which spread to the cortex, causing progressive synaptic dysfunction and neurodegeneration. Ultimately, this process results in cognitive decline and the development of dementia. The target population for treatment with these disease-modifying drugs is patients with mild cognitive impairment (MCI) or mild dementia but not patients with advanced dementia.

More recently, the therapeutic focus of disease-modifying drugs has been directed to elderly population in earlier stages of AD. For example, the AHEAD 3–45 trial (NCT04468659) [4] is a clinical trial of lecanemab for asymptomatic elderly population with amyloid positivity (A+); A+ corresponds to the condition defined as the Alzheimer's continuum in the 2018 National Institute on Aging and Alzheimer's Association (NIA-AA) research framework [5]. The Alzheimer's continuum based on the NIA-AA criteria includes three categories: Amyloid and tau positivity (A+T+) is defined as "Alzheimer's disease", and amyloid positivity and tau negativity (A+T−) is defined as "Alzheimer's pathologic change" if neurodegeneration is not present or "Alzheimer's and concomitant suspected non-Alzheimer's pathologic change" if neurodegeneration is present. Among these categories, preclinical AD (A+T+) is receiving more attention because it is associated with faster cognitive decline and a higher risk of progression to MCI than A−T− and A+T− [6, 7].

Determining how long and to what extent brain atrophy progresses in the elderly population on the preclinical Alzheimer's continuum would contribute to a better understanding of the pathophysiology of neurodegeneration and a more accurate interpretation of the results of clinical trials of individuals on the Alzheimer's continuum. Although several research groups have already reported accelerated cerebral atrophy in subjects with A+T+ compared with subjects with A−T− [8–10], the average observation period for these studies was short at approximately two years. Longitudinal structural magnetic resonance imaging (MRI) can estimate the extent of brain atrophy over time before the first clinical manifestations of AD appear [11], but few studies with long follow-up periods (more than 4–5 years) have reported how long and to what extent brain atrophy is accelerated in elderly individuals on the preclinical Alzheimer's continuum.

The hypothesis of this study was that the elderly population on the preclinical Alzheimer's continuum have accelerated brain atrophy compared with those with amyloid and tau negativity (A−T−). Longitudinal analysis of structural MRI and cognitive performance and survival analysis of progression to MCI or dementia were performed on four groups consisting of both positive and negative combinations of A and T biomarkers, which are neuropathological features of AD, using long-term follow-up data.

Methods

Participants

The Alzheimer's Disease Neuroimaging Initiative (ADNI) was launched in 2003 as a public–private partnership, led by principal investigator Michael W. Weiner, MD. The primary goal of ADNI has been to test whether serial MRI, PET, other biological markers, and clinical and neuropsychological assessment can be combined to measure the progression of MCI and early AD.

In the present study, 367 participants who had cerebrospinal fluid (CSF) Aβ42 and phosphorylated tau 181 (p-tau181) data were drawn from the ADNI 1, 2, GO, and 3 datasets. We used the following data with the last visit on 2022–02-22 from the ADNI website: ADNI-MERGE.csv. All the participants in the present study were diagnosed as cognitively normal at baseline. They had baseline scores of 24 to 30 on the Mini-Mental State Examination (MMSE) [12] and global scores of 0 on the Clinical Dementia Rating (CDR) [13]. Their scores on the Wechsler Memory Scale-Revised (WMS-R) Logical Memory II [14] were based on the number of years of education: ≥ 3 for education of 0 to 7 years, ≥ 5 for 8 to 15 years, and ≥ 9 for ≥ 16 years. If a participant had a significant subjective memory concern, it was reported by the participant, study partner, or clinician. All participants were followed up six months after baseline, one year, and every year beyond. A flow diagram showing the process of participant selection for this study is presented in Fig. 1.

Diagnostic group assignment based on amyloid and tau positivity/negativity by CSF biomarker measurements

CSF concentrations of Aβ42 and p-tau181 were measured with the Elecsys immunoassays using the cobas e601 analyzer (Roche Diagnostics GmbH, Mannheim, Germany) [15, 16]. In the present study, the cutoff values for CSF concentrations of Aβ42 and p-tau181 were defined as 981 pg/mL based on 18F-florbetapir PET and
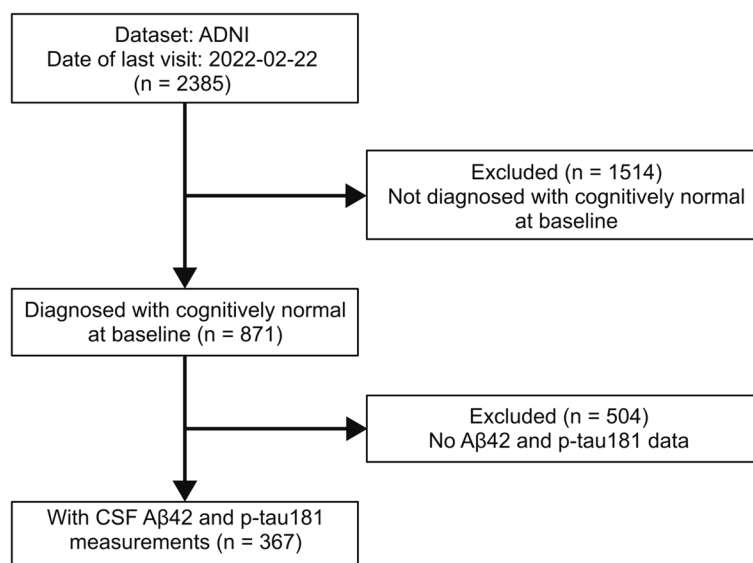
Fig. 1 Flow diagram of the participant selection from the ADNI dataset. Abbreviations: Aβ42 = amyloid-beta 42; ADNI = Alzheimer's Disease Neuroimaging Initiative; CSF = cerebrospinal fluid; p-tau181 = phosphorylated tau 181

24.3 pg/mL based on 18F-flortaucipir PET, respectively [17]; namely, participants with Aβ42 < 981 pg/mL were classified as amyloid positive (A+). Participants with p-tau181 > 24.3 pg/mL were classified as tau positive (T+).

MRI acquisition and processing

Image registration of serial T1-weighted (T1w) MRI scans

All the participants had undergone more than one T1w MRI scan on a 1.5-T or 3-T scanner. The imaging protocols were described by Jack et al. [18]. All the serial T1w MRI scans were corrected for intensity inhomogeneity with N4ITK [19] following noise reduction with nonlocal means [20]. The baseline scan was then rigidly registered to the ADNI template with NiftyReg [21, 22]. The ADNI template was created from T1w MRI scans of 52 cognitively normal participants with antsMultivariateTemplateConstruction.sh script implemented in ANTs [23, 24]. All the follow-up scans were affinely registered to the baseline scan rigidly registered to the template with NiftyReg. The averaged image was created from the registered serial scans. Finally, all the serial scans were affinely registered to the averaged scan with NiftyReg. The image registration described here is depicted in Fig. 2.

Computation of cerebral cortical thickness

Regional cerebral thickness was computed from the serial scans affinely registered to the averaged image above with DL + DiReCT [25]. DL + DiReCT is a method combining deep learning (DL)-based neuroanatomical segmentation

and cortex parcellation with diffeomorphic registration-based cortical thickness (DiReCT) measurement [26]. We computed the voxel-weighted average of the mean cortical thickness within the bilateral entorhinal, fusiform, inferior temporal, and middle temporal regions defined by the Desikan-Killiany parcellations [27]. These regions were derived from the AD-signature regions of interest [28]. The cortical thickness computation described here is depicted in Fig. 2.

Computation of k-means normalized boundary shift integral (KN-BSI)

To compute volume changes in the hippocampus, lateral ventricle, and whole brain on individual serial MRI scans, KN-BSI [29] was adopted. The hippocampal labels were automatically segmented with hippodeep [30] from the registered serial scans (Fig. 1). The lateral ventricle and whole brain labels were extracted from the segmentations created by DL + DiReCT above (Fig. 2). Symmetric differential bias correction (DBC) [31, 32] was applied to the serial scans to correct the differences in intensity inhomogeneity among the serial scans. A median filter with a radius of five voxels for DBC was adopted with the original reference [32]. Volume changes in the lateral ventricle and whole brain were computed with normal KN-BSI from the DBC-corrected scans. In contrast, volume changes in the hippocampus were computed with a double intensity-window KN-BSI to capture boundary shift at both the hippocampus-CSF border and the hippocampus-white matter border [33] from the DBC-corrected scans. The volume at each timepoint was calculated by
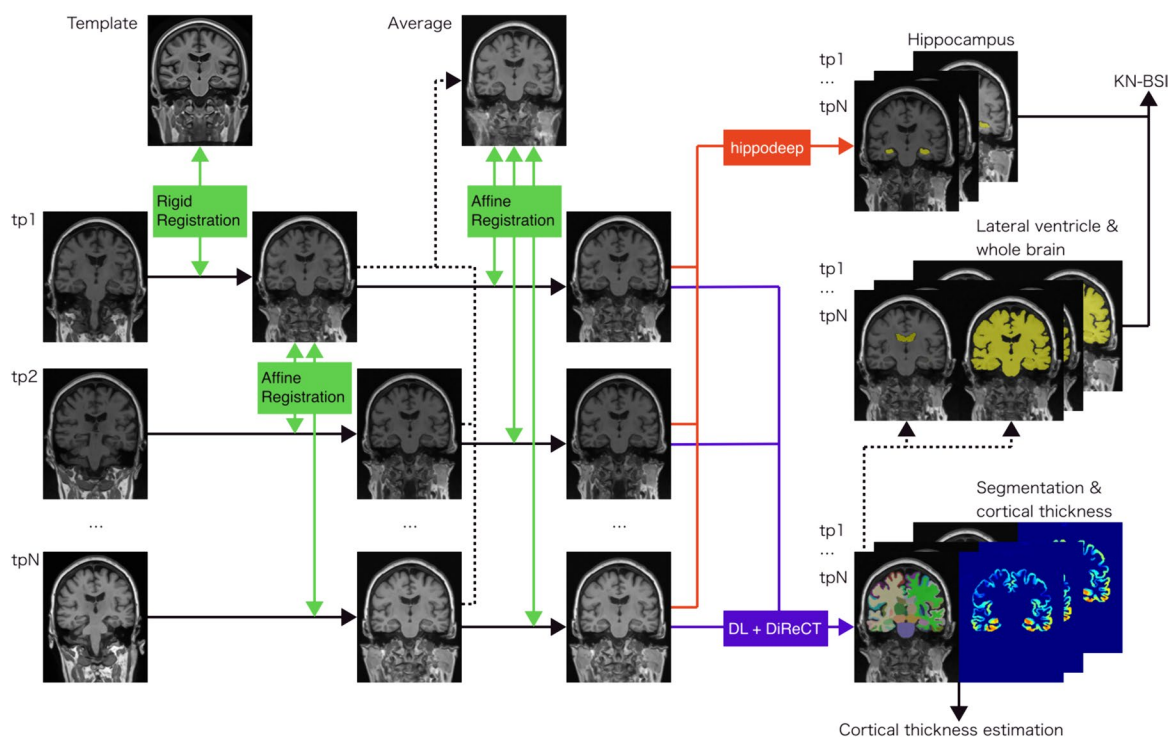
Fig. 2 Image processing pipeline for the KN-BSI and cortical thickness computation. First, T1w scans at each timepoint were affinely registered to the baseline scan that had been rigidly registered to the ADNI template. Second, an averaged image was generated from the affinely registered scans at each timepoint. Third, T1w scans at each timepoint were affinely registered to the averaged image. DL + DiReCT was applied to the affinely registered image at each time point for segmentation and cortical thickness estimation. Segmentations for the whole brain and lateral ventricle were generated from the resultant images from DL + DiReCT. Hippocampal segmentations were generated using hippodeep. Finally, KN-BSI was computed for longitudinal volume changes in the whole brain, lateral ventricle, and hippocampus using the affinely registered images and segmentations. Abbreviations: KN-BSI, k-means normalized boundary shift integral; DL + DiReCT, deep learning-based neuroanatomical segmentation + diffeomorphic registration-based cortical thickness; tpN, Nth timepoint

subtracting the volume change between the baseline and each timepoint as calculated by KN-BSI from the volume at the baseline.

Cognitive assessment
We adapted the Preclinical Alzheimer Cognitive Composite (PACC) to assess subtle cognitive changes for cognitively normal participants with A + and/or T + status. The PACC in the current study was a baseline standardized z score composite of the Delayed Word Recall score from the Alzheimer's Disease Assessment Scale—Cognitive Subscale, the Delayed Recall score on the Logical Memory IIA subtest from the WMS-R, the MMSE, and log-transformed Trail-Making Test B Time to Completion [34]. Note that the PACC score decreases with worse cognitive performance.

Statistical analyses
Descriptive statistics were calculated for the data obtained in this study. They are presented as means and standard deviations for continuous quantities and as frequencies and proportions for categorical variables. The CSF concentrations of $A\beta42 < 200$ pg/mL and $> 1,700$ pg/mL were set as 200 pg/mL and 1,700 pg/mL, respectively, for the statistics because CSF Aß42 had the lower and upper technical limits of measurement of < 200 mg/mL and 1,700 pg/mL, respectively. Similarly, the CSF concentrations of tau < 80 pg/mL and p-tau181 < 8 pg/mL were set as 80 pg/mL and 8 pg/mL, respectively, for the statistics because CSF tau and CSF p-tau181 had lower technical limits of the measurement of < 80 mg/mL and 8 pg/mL, respectively.

Outcome changes for each of the four groups assigned by amyloid and tau positivity/negativity were analyzed using a generalized linear mixed-effects model. The following five variables were selected as response variables: whole brain volume, lateral ventricular volume, hippocampal volume, cortical thickness in the AD-signature regions of interest, and the PACC score. The linearity of the relationships between outcome and time was assessed by locally estimated scatterplot smoothing (LOESS) [35]. Figure 3 shows the LOESS plots for
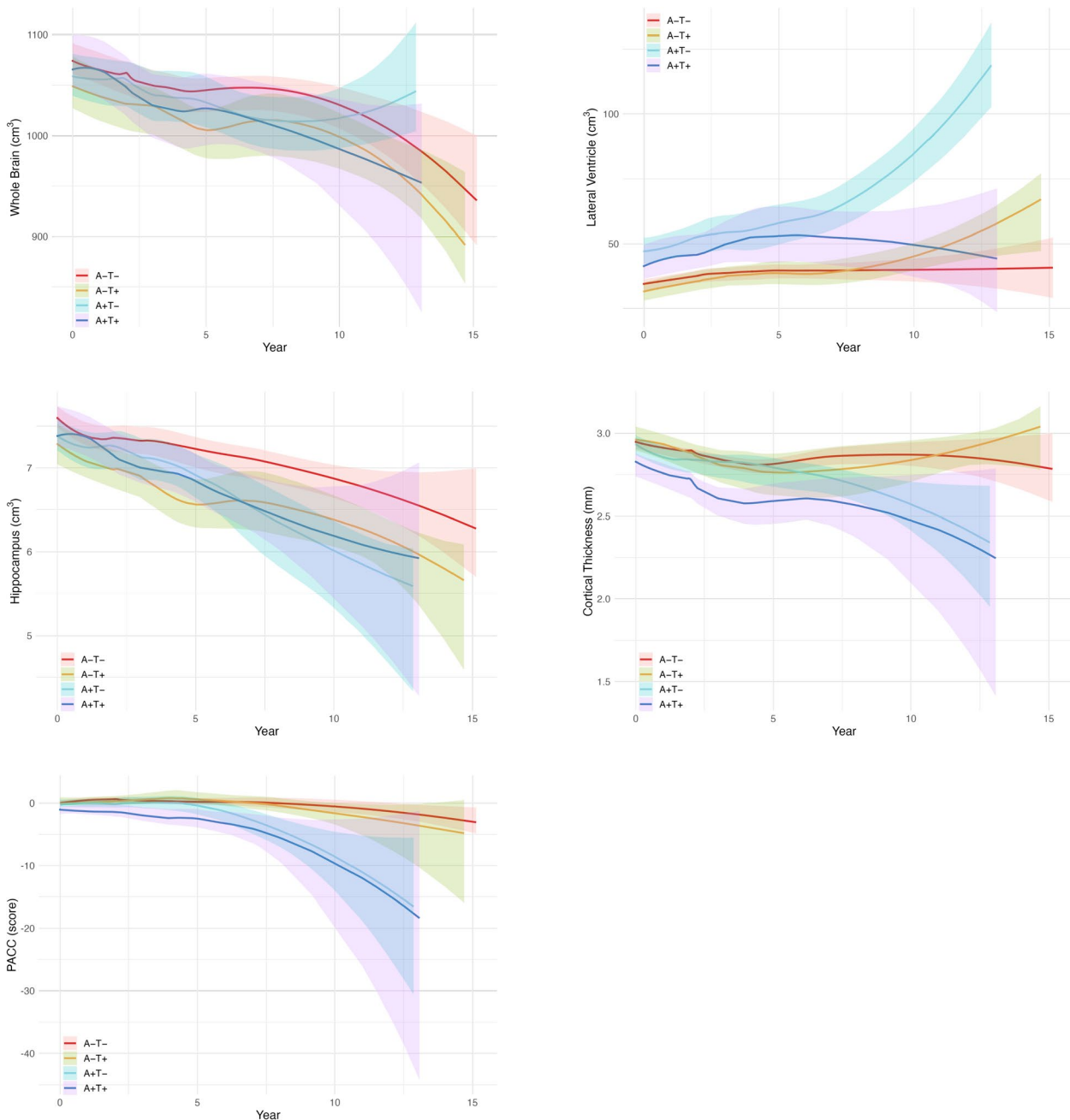
Fig. 3 Mean measurement trajectories and 95% confidence bands using LOESS for each group classified by amyloid and tau positivity/negativity. Abbreviations: A − = amyloid negative; A + = amyloid positive; LOESS = locally estimated scatterplot smoothing; PACC = Preclinical Alzheimer Cognitive Composite; T − = tau negative; T + = tau positive

the response variables in the four groups. In addition, 95% confidence bands calculated by bootstrapping with 10,000 resamples were added to the graph. Based on the linear trends delineated by these plots, we determined to use a generalized linear mixed-effects model with a linear term for time of up to 7.5 years from the baseline as the main analysis. Models that included quadratic terms

were also examined and compared using the Akaike Information Criterion (AIC) [36] to assess the goodness of fit of the data (Supplementary Table 1). Although the AIC results were better for the models that included quadratic terms, a linear model was adopted due to ease of interpretability. Due to the very small amount of data obtained after 7.5 years in this study, these data were

excluded from the main analysis. Furthermore, two sensitivity analyses were conducted: First, a generalized linear mixed-effects model incorporating additional interactions between covariates and time was employed to examine these interactions. Second, a generalized linear mixed-effects model was used to analyze the data harmonized for variability between different MR scanners. The harmonization was applied to the MRI measurements using the longCombat package [37] in R version 4.2.1 (R Foundation for Statistical Computing, Vienna, Austria) to alleviate non-biological variations in data acquired from multiple MR scanners with magnetic field strengths of 1.5 T and 3 T across multiple research sites. The explanatory variables selected were the group (A−T−group as the reference), time (in years), the interaction term between the group and time, and candidate confounders (presence of subjective memory concerns, age at baseline, sex, number of years of education, and number of *APOE* ε4 alleles). For analyses where the response variable was either the whole brain volume, lateral ventricular volume, or hippocampal volume, intracranial volume at baseline from ADNIMERGE.csv was also included as a confounding factor. These confounding factors were determined in previous studies [38, 39]. Each of the mixed-effects model assumed a random intercept and random slope at the individual level, modeling that each measurement was nested in individuals. The overall group effect was tested using a likelihood ratio test comparing the full model to a reduced model, excluding the group variable. If the test was found to be significant, under the predictions calculated by this model, modeled means were calculated for each group and each year, and approximate curves were drawn using fractional polynomial regressions.

In the sub-analysis, the same analysis as the main analysis was performed using all data (i.e., including 7.5 years and beyond). Based on visual inspection of the LOESS plots (Fig. 3), we also included the quadratic term for time and interaction terms between the group and the quadratic term for time in the generalized linear mixed-effects model. As in the main analysis, the overall group effect was tested using a likelihood ratio test comparing the full model to a reduced model, excluding the group variable. In addition, the same analysis was performed on the data harmonized using longCombat for the MRI measurements as a sensitivity analysis.

Next, survival analysis was performed for conversion to MCI or dementia using data from the entire period. Kaplan–Meier curves were drawn for each group and compared by the log-rank test. The Cox proportional hazards model with the group as the explanatory variable was then used to calculate the hazard ratio and its 95% confidence interval for the A−T−group as a reference. First, the unadjusted model was applied. Second, the

multivariable model was adjusted for baseline age, sex, number of years of education, *APOE* ε4 status, and presence of subjective memory concerns.

All tests were two-tailed, and *p*-values less than 0.05 were considered statistically significant. This study was an exploratory analysis; therefore, no alpha adjustment was made to control for Type 1 errors. Stata 18/MP (Stata Crop LLC, College Station, TX, USA) was used for the analysis. LOESS graphs were drawn using ggplot2 in R.

Results

Demographic characteristics

Among 367 participants in the study, the mean (standard deviation) age was 73.8 (5.9) years, and the observation period was 5.1 (3.4) years; there were 174 male (47.4%) and 193 female (52.6%) participants. Approximately 13.1% (48/367) of participants were classified as A+T+using CSF concentrations of Aβ42 and p-tau181, compared with 23.4% (86/367) as A+T−, 17.2% (63/367) as A−T+, and 46.3% (170/367) as A−T−. Further demographic characteristics are depicted in Table 1.

Changes in longitudinal structural MRI measurements and PACC scores over time

Main analysis up to 7.5 years from the baseline

Figure 4 reveals modeled mean profiles for the volumes of the whole brain, lateral ventricle, and hippocampus, cortical thickness in the AD-signature regions of interest, and PACC scores in the four groups from baseline to 7.5 years based on a generalized linear mixed-effects model. Three cases (two A−T+ and one A+T−) had no data at baseline. This model was controlled for the covariates including baseline age, *APOE* ε4 status (0, 1, or 2), sex, number of years of education, and baseline intracranial volume (only for the volumetric measures). The likelihood ratio test for the group effect was significant for the whole brain ($\chi2(6) = 27.0$; $P < .001$), lateral ventricle ($\chi2(6) = 78.9$; $P < .001$), hippocampus ($\chi2(6) = 19.0$; $P = .004$), cortical thickness ($\chi2(6) = 29.2$; $P < .001$), and PACC score ($\chi2(6) = 32.8$; $P < .001$). Since these likelihood ratio tests were significant, we determined that including group variables in the statistical model was necessary.

For the whole brain and hippocampal volume and cortical thickness, only the A+T+ group showed statistically significantly greater volume loss and cortical thinning over time than the A−T− group ($\beta = −2.782$ cm^3/year, 95% confidence interval (CI) = −4.060 to −1.504, $P < .001$ for the whole brain volume, $\beta = −0.057$ cm^3/year, 95% CI = −0.085 to −0.029, $P < .001$ for the hippocampal volume, and $\beta = −0.02$ mm/year, 95% CI = −0.03 to −0.01, $P < .001$ for the cortical thickness; Figure 4a, c, d, and Table 2). For

Table 1 Participant characteristics by amyloid and tau positivity/negativity classification

	A+T+ (n = 48)	A+T− (n = 86)	A−T+ (n = 63)	A−T− (n = 170)
Baseline Characteristics				
Age, mean (SD), y	76.3 (5.1)	73.4 (5.9)	75.8 (6.6)	72.6 (5.5)
No. of male (%)	21 (44)	40 (47)	28 (44)	85 (50)
Education, mean (SD), y	16.2 (2.5)	16.4 (2.7)	16.5 (2.7)	16.3 (2.6)
Ethnicity (%)				
Not Hispanic/Latino	47 (98)	84 (98)	61 (97)	160 (94)
Hispanic/Latino	1 (2)	2 (2)	1 (2)	8 (5)
Unknown	0 (0)	0 (0)	1 (2)	2 (1)
Race (%)				
American Indian/Alaskan native	0 (0)	1 (1)	0 (0)	0 (0)
Asian	0 (0)	1 (1)	1 (2)	2 (1)
Black	2 (4)	8 (9)	1 (2)	13 (8)
White	46 (96)	72 (84)	61 (97)	154 (91)
More than one race	0 (0)	4 (5)	0 (0)	1 (1)
Subjective memory concern (%)	13 (27)	17 (20)	17 (27)	48 (28)
APOEε4 allele = 1 (%)	25 (52)	29 (34)	13 (21)	27 (16)
APOEε4 allele = 2 (%)	2 (4)	6 (7)	0 (0)	1 (1)
PACC, mean (SD)	−0.97 (2.41)	−0.30 (2.80)	−0.10 (2.72)	0.07 (2.33)
MMSE, mean (SD)	29.1 (1.2)	29.1 (1.1)	28.9 (1.3)	29.1 (1.1)
CDR-SB (%)				
0	43 (90)	76 (88)	58 (92)	161 (95)
0.5	4 (8)	10 (12)	5 (8)	9 (5)
1	1 (2)	0 (0)	0 (0)	0 (0)
CSF $A\beta_{42}$, mean (SD), pg/mL	706.8 (177.8)[a]	689.9 (203.2)	1548.5 (226.8)[b]	1479.3 (230.3)[b]
CSF tau, mean (SD), pg/mL	346.5 (73.9)	173.1 (49.2)[c]	349.2 (69.1)	197.6 (39.9)
CSF p-tau$_{181}$, mean (SD), pg/mL	35.5 (8.7)	16.0 (4.7)[d]	31.3 (6.8)	17.3 (3.5)
Whole brain volume, mean (SD), cm^3	1061.949 (94.060)	1059.643 (102.777)	1045.114 (96.797)	1073.724 (109.641)
Ventricular volume, mean (SD), cm^3	39.782 (19.863)	47.447 (24.799)	31.686 (14.950)	34.223 (14.294)
Hippocampal volume, mean (SD), cm^3	7.360 (0.846)	7.395 (0.943)	7.291 (0.976)	7.607 (0.920)
Cortical thickness, mean (SD), mm	2.84 (0.25)	2.92 (0.28)	2.95 (0.26)	2.95 (0.21)
Follow-up characteristics				
Follow-up, mean (SD), y	4.4 (3.1)	4.5 (3.0)	5.6 (3.7)	5.5 (3.5)
Follow-up CSF measurements available (%)	32 (67)	44 (51)	29 (46)	107 (63)
Progression to amyloid-positive (%)	NA	NA	6 (10)	14 (8)
Progression to tau-positive (%)	NA	7 (8)	NA	10 (6)
Progression to dementia (%)	6 (12)	5 (6)	4 (6)	3 (2)

Abbreviations: *CDR-SB* Clinical Dementia Rating Sum of Boxes, *CSF* Cerebrospinal fluid, *MMSE* Mini-Mental State Examination, *NA* Not applicable, *PACC* Preclinical Alzheimer Cognitive Composite, *SD* Standard deviation

[a] Concentration of CSF $A\beta_{42}$ < 200 pg/mL was set as 200 pg/mL for the statistics due to the lower technical limit of the measurement

[b] Concentration of CSF $A\beta_{42}$ > 1700 pg/mL was set as 1700 pg/mL for the statistics due to the upper technical limit of the measurement

[c] Concentration of CSF tau < 80 pg/mL was set as 80 pg/mL for the statistics due to the lower technical limit of the measurement

[d] Concentration of CSF p-tau$_{181}$ < 8 pg/mL was set as 8 pg/mL for the statistics due to the lower technical limit of the measurement

the lateral ventricular volume, the A+T− and A+T+ groups showed statistically significantly greater volume expansion over time than the A−T− group (β = 0.757 cm^3/year, 95% CI = 0.463 to 1.050, *P* < .001 for A+T− vs. A−T−, and β = 0.889 cm^3/year, 95% CI = 0.523 to 1.255, *P* < .001 for A+T+ vs. A−T−; Figure 4b and Table 2). For the PACC score, the A+T+ and A+T− groups showed statistically significantly greater cognitive decline over time than the A−T− group (β = −0.19/year, 95% CI = −0.36 to −0.02, *P* =
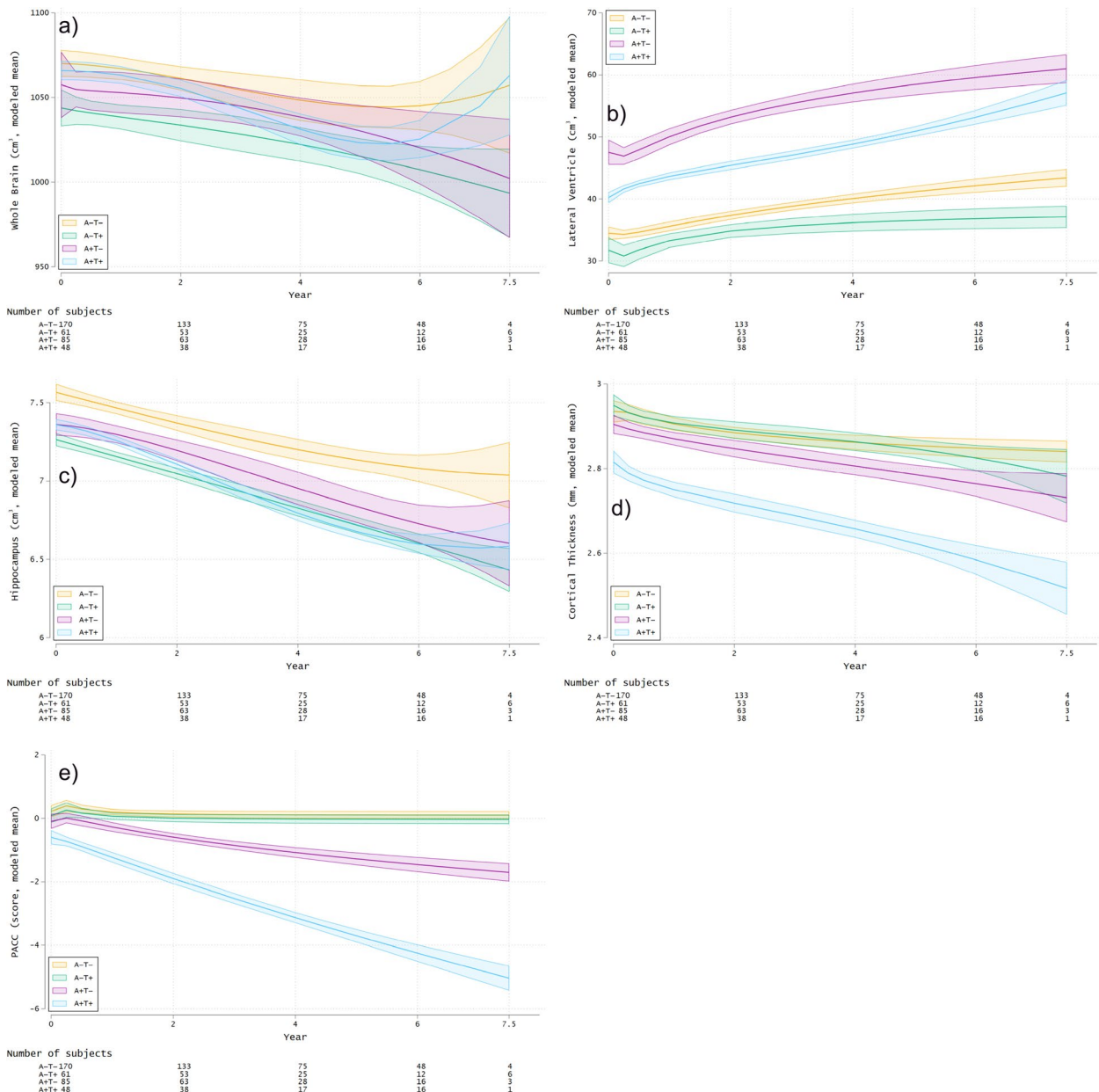
Fig. 4 Changes in longitudinal MRI measurements and cognitive performance by amyloid and tau positivity/negativity classification over 7.5 years. **a-e** Trajectories of modeled mean profiles of whole brain volume, lateral ventricular volume, hippocampal volume, cortical thickness, and PACC scores based on a generalized linear mixed-effects model and 95% confidence bands. The models were controlled for baseline age, *APOE* ε4 status, sex, number of years of education, and baseline intracranial volume (only for the volumetric measures). Abbreviations: A − = amyloid negative; A + = amyloid positive; PACC = Preclinical Alzheimer Cognitive Composite; T − = tau negative; T + = tau positive

.029 for A+T− vs. A−T−, and β = −0.59/year, 95% CI = −0.80 to −0.37, *P* < .001 for A+T+ vs. A−T−; Figure 4e and Table 2). Furthermore, based on these 95% CIs, the A+T+ group showed statistically significantly greater decline in cognitive function over time than the A+T− group (Table 2). The A−T+ group did not show greater brain atrophy and cognitive decline

than the A−T− group based on MRI measures and the PACC scores, respectively. The main effects (group differences at Time = 0) are shown in the Group row in Table 2. A consistent trend was also confirmed in the model with additional covariate and time interactions as a sensitivity analysis (Supplementary Table 2). In the model, significant associations were observed

Table 2 Summary of a generalized linear mixed-effects model in the main analysis for serial structural MRI and cognitive performance measures from baseline to 7.5 years

	Whole brain			Lateral ventricle			Hippocampus		
	β	95% CI Lower, Upper	P-value	β	95% CI Lower, Upper	P-value	β	95% CI Lower, Upper	P-value
Intercept	1353.323	1281.298, 1425.348	<.001	−21.463	−41.046, −1.880	.032	11.707	10.577, 12.838	<.001
Age	−4.239	−5.108, −3.370	<.001	0.767	0.532, 1.002	<.001	−0.051	−0.065, −0.037	<.001
Male	16.673	4.900, 28.447	.006	−1.893	−5.077, 1.290	.244	0.102	−0.083, 0.287	.280
Years of education	−0.349	−2.261, 1.563	.720	0.194	−0.322, 0.710	.462	−0.039	−0.069, −0.009	.012
APOE ε4 alleles	16.491	−3.813, 36.795	.111	−8.790	−14.296, −3.283	.002	0.083	−0.236, 0.402	.609
Baseline ICV	0.541	0.504, 0.577	<.001	0.042	0.032, 0.052	<.001	0.003	0.002, 0.003	<.001
SMC	14.324	2.965, 25.682	.013	2.182	−0.916, 5.280	.168	0.067	−0.111, 0.245	.461
Group									
A−T+	5.763	−8.256, 19.782	.420	−3.720	−8.059, 0.619	.093	−0.028	−0.248, 0.192	.802
A+T−	−16.684	−29.442, −3.925	.010	13.526	9.590, 17.462	<.001	−0.168	−0.368, 0.033	.101
A+T+	−2.018	−18.274, 14.238	.808	4.370	−0.609, 9.350	.085	−0.055	−0.310, 0.200	.673
Time	−5.878	−6.450, −5.306	<.001	1.239	1.072, 1.406	<.001	−0.091	−0.103, −0.078	<.001
Group × time									
A−T+ × time	−0.321	−1.441, 0.800	.575	−0.038	−0.363, 0.287	.819	−0.023	−0.047, 0.002	.069
A+T− × time	−0.524	−1.548, 0.500	.316	0.757	0.463, 1.050	<.001	−0.015	−0.038, 0.007	.188
A+T+ × time	−2.782	−4.060, −1.504	<.001	0.889	0.523, 1.255	<.001	−0.057	−0.085, −0.029	<.001

	Cortical thickness			PACC		
	β	95% CI Lower, Upper	P-value	β	95% CI Lower, Upper	P-value
Intercept	4.19	3.87, 4.51	<.001	6.65	3.52, 9.78	<.001
Age	−0.02	−0.02, −0.01	<.001	−0.13	−0.17, −0.09	<.001
Male	−0.08	−0.12, −0.03	.001	−1.21	−1.65, −0.77	<.001
Years of education	0.00	−0.01, 0.01	.602	0.30	0.22, 0.39	<.001
APOE ε4 alleles	−0.01	−0.10, 0.08	.808	−0.41	−1.31, 0.48	.366
Baseline ICV	NA	NA	NA	NA	NA	NA
SMC	0.05	−0.00, 0.10	.057	−0.75	−1.27, −0.23	.005
Group						
A−T+	0.06	−0.01, 0.12	.075	0.16	−0.46, 0.78	.619
A+T−	−0.02	−0.08, 0.04	.520	−0.31	−0.87, 0.26	.287
A+T+	−0.06	−0.13, 0.01	.104	−0.34	−1.06, 0.38	.356
Time	−0.02	−0.02, −0.01	<.001	−0.01	−0.10, 0.09	.852
Group × time						
A−T+ × time	−0.01	−0.02, 0.00	.083	−0.08	−0.27, 0.11	.388
A+T− × time	−0.00	−0.01, 0.00	.349	−0.19	−0.36, −0.02	.029
A+T+ × time	−0.02	−0.03, −0.01	<.001	−0.59	−0.80, −0.37	<.001

Abbreviations: *CI* Confidence interval, *ICV* Intracranial volume, *NA* Not applicable, *PACC* Preclinical Alzheimer Cognitive Composite, *SMC* Subjective memory concern

between the baseline age and longitudinal changes in the expansion of the lateral ventricles, cortical thinning, and lower PACC scores (Supplementary Table 2). In the sensitivity analysis of the data harmonized for MRI measurements using longCombat, the model yielded consistent results with those obtained from the analysis of non-harmonized data (Supplementary Table 3 and Supplementary Figure 1).

Sub-analysis using data from the entire period

Supplementary Figure 2 shows the modeled mean profiles for the MRI measurements and PACC scores including the quadratic term for time and interaction terms between the group and the quadratic term for time in the four groups for the entire period. The likelihood ratio test for the group effect was significant for whole brain ($\chi 2(9) = 32.7$; $P < .001$), lateral ventricle ($\chi 2(9) = 81.6$; $P < .001$),

hippocampus ($\chi2(9) = 27.5$; $P = .001$), cortical thickness ($\chi2(9) = 36.3$; $P < .001$), and PACC scores ($\chi2(9) = 48.1$; $P < .001$). Since these likelihood ratio tests were significant, we determined that including group variables in the statistical model was necessary.

For the whole brain volume and cortical thickness, only the A+T+ group showed statistically significantly greater volume loss and cortical thinning over time than the A−T− group ($\beta = -2.598$ cm³/year, 95% CI = −4.997 to −0.200, $P = .034$ for the whole brain volume, and $\beta = -0.02$ mm/year, 95% CI = −0.04 to −0.01, $P = .010$ for the cortical thickness; Supplementary Figure 2a and Figure 2d and Supplementary Table 4), but no groups showed evidence of acceleration in atrophy rates compared with the reference A−T− group. For the lateral ventricular volume, the A+T− and A+T+ groups showed statistically significantly greater volume expansion than the reference A−T− group ($\beta = 0.634$ cm³/year, 95% CI = 0.253 to 1.016, $P = .001$ for A+T− vs. A−T−, and $\beta = 1.026$ cm³/year, 95% CI = 0.547 to 1.505, $P < .001$ for A+T+ vs. A−T−; Supplementary Figure 2b and Supplementary Table 4), but no groups showed evidence of acceleration in atrophy rates compared with the reference A−T− group. For the hippocampal volume, only the A+T− group showed a statistically significant acceleration in atrophy rates compared with the reference A−T− group ($\beta = -0.011$ cm³/year², 95% CI = −0.019 to −0.004, $P = .003$; Supplementary Figure 2c and Supplementary Table 4). For the PACC score, the A+T− and A+T+ groups showed a statistically significant acceleration in cognitive decline compared with the reference A−T− group ($\beta = -0.05$/year², 95% CI = −0.10 to −0.01, $P = .023$ for A+T− vs. A−T−, and $\beta = -0.12$/year², 95% CI = −0.18 to −0.06, $P < .001$ for A+T+ vs. A−T−; Supplementary Figure 2e and Supplementary Table 4). In the sensitivity analysis of the data harmonized using longCombat, the A−T+, A+T−, and A+T+ groups all showed an accelerated rate of cortical thinning relative to the reference A−T− group; however, the extent of this acceleration was minor, and differences were notable only beyond the third decimal place (Supplementary Figure 3d and Supplementary Table 5). Regarding the whole brain volume, no group showed a significantly greater reduction over time than the reference A−T− group (Supplementary Figure 3a and Supplementary Table 5). The other results revealed no substantial differences compared with the results using the non-harmonized data.

Survival analysis for conversion to MCI or dementia

Of the 367 participants, 12 had only one observation and were not included in the survival analysis. Therefore, we analyzed 355 participants in the survival analysis. The number of outcome occurrences was 75; of these, 70 were MCI, and 5 were dementia. The mean follow-up time for the two groups was not significantly different at 4.36 years and 8.72 years for the MCI and dementia groups, respectively, (Welch's t-test two-sided $P=.080$). Proportional hazards were confirmed by testing the proportional hazard assumption, which revealed no violation of the assumption (unadjusted model: $P=.982$, adjusted model: $P=.902$). Spearman's correlation coefficient between the explanatory variables in the adjusted model was at most 0.310 (Group and *APOE* ε4 alleles); therefore, multicollinearity is unlikely. Kaplan–Meier curves showing survival from conversion to MCI or dementia in the four groups are depicted in Fig. 5. The survival curves showed a difference across the four groups (log-rank test, $P=.001$). A Cox proportional hazard analysis revealed that the A+T+ and A+T− groups had an increased risk of conversion to MCI or dementia compared with the reference A−T− group in the unadjusted models (hazards ratio=4.03, 95% CI: 2.17–7.49, $P<.001$ for A+T+ vs. A−T−, and hazards ratio=2.58, 95% CI: 1.39–4.77, $P=.003$ for A+T− vs. A−T−; Table 3). We also found that the A+T+ and A+T− groups had a significantly increased risk of conversion to MCI or dementia in the adjusted models (hazards ratio=3.35, 95% CI: 1.76–6.39, $P<.001$ for A+T+ vs. A−T−, and hazards ratio=2.38, 95% CI: 1.26–4.48, $P=.007$ for A+T− vs. A−T−; Table 3). There was no significant difference in survival curves for the A−T+ group compared with the A−T− group in the unadjusted and adjusted models.

Discussion

Main findings

The findings of this longitudinal study demonstrated that amyloid positivity (A+) accelerates lateral ventricular expansion, while concurrent positivity for both amyloid and tau (A+T+) precipitates cerebral atrophy affecting the whole brain, hippocampus, and cerebral cortex in the AD-signature regions in cognitively normal elderly individuals. Furthermore, it concomitantly leads to a steep decrement in cognitive performance. Conversely, A−T+ does not engender cerebral atrophy or cognitive decline. Additional survival analysis over the entire observation period indicated that A+T+ and A+T− augment the subsequent risk for MCI and dementia.

Interpretation and comparison with previous studies

The results of the main analysis using a generalized linear mixed-effects model in our longitudinal study suggest that A+ alone promotes lateral ventricular expansion and that cerebral atrophy becomes more extensive when combined with T+. Desikan et al., Xie et al., and Costoya-Sánchez et al. have already reported accelerated atrophy
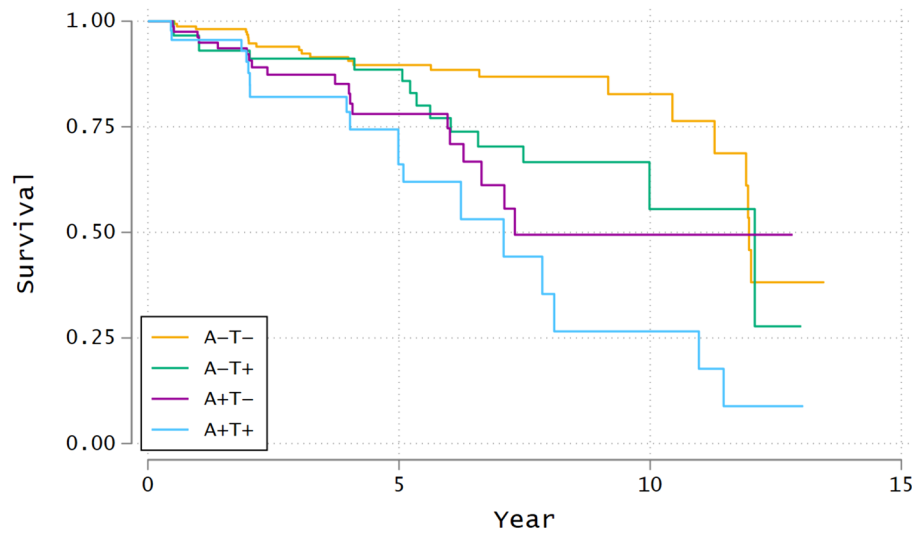
Number at risk

A−T−	165	83	14	0
A−T+	60	33	5	0
A+T−	84	28	1	0
A+T+	46	16	3	0

Fig. 5 Kaplan–Meier curves on progression to MCI or dementia according to amyloid and tau positivity/negativity. Abbreviations: A − = amyloid negative; A + = amyloid positive; T − = tau negative; T + = tau positive

Table 3 Cox proportional hazard ratios for conversion to mild cognitive impairment or dementia

Characteristic	Subgroup	n	Hazards ratio	95% CI		P-value
				Lower	Upper	
Unadjusted model						
Group	A−T+	60	1.85	0.96	3.55	.064
	A+T−	84	2.58	1.39	4.77	.003
	A+T+	46	4.03	2.17	7.49	<.001
Adjusted model						
Group	A−T+	60	1.75	0.89	3.44	.106
	A+T−	84	2.38	1.26	4.48	.007
	A+T+	46	3.35	1.76	6.39	<.001
Age			1.06	1.02	1.11	.005
Male			1.54	0.94	2.51	.084
Years of education			0.94	0.87	1.02	.160
APOE ε4 alleles			2.19	0.96	5.00	.063
SMC			1.26	0.69	2.29	.446

Abbreviations: *CI* Confidence interval, *SMC* Subjective memory concern

in subjects with A + T + compared with that in subjects with A − T − in the cerebral cortex and hippocampal subregions [8–10]. Our results are consistent with the findings of these studies. Similar to our study, these studies used the ADNI data, and Costoya-Sánchez et al. additionally used data from other longitudinal studies, but their average observation period was approximately two years.

In our study, we analyzed data from a longer observation period than these studies and added new longitudinal findings from the whole brain and lateral ventricular volumes and cortical thickness including both the medial and lateral temporal regions, supporting the notion that A + T + accelerates brain atrophy in the regions related to AD.

Notably, unlike the A + T + and A − T + groups, the A + T − group showed expansion of the lateral ventricles at baseline compared with the A − T − group. The reason for this is unclear. Given that lateral ventricular expansion is not specific to AD, it is possible that the A + T − group included a higher proportion of subjects with non-AD causes of lateral ventricular expansion, such as dementia with Lewy bodies [40, 41], or increased white matter hyperintensity volume [42]. During the follow-up period, similar to the A + T + group, the A + T − group exhibited accelerated lateral ventricular expansion compared to the A − T − group. A study on autopsy cases revealed that 50–73% of cases classified as A + T − based on CSF Aβ42 and p-tau181 were found to have AD pathology [43]. For this reason, it should be considered that within the A + T − group in our study, there may be cases in which the T classification determined by p-tau181 could have been a false negative. It is ultimately difficult to ascertain whether the underlying cause of the accelerated lateral ventricular expansion in the A + T − group is due to factors associated with non-AD pathology or whether it is related to amyloid positivity or tau positivity. In addition, the high contrast between the brain parenchyma and CSF may have provided a more reliable longitudinal measurement of the lateral ventricle than those of the other MRI measurements [44], which could have facilitated detection of accelerated lateral ventricular expansion.

With respect to global cognitive performance, our results in the main analysis indicate that A + promotes cognitive decline and that the addition of T + further promotes cognitive decline. There is recent documentation of A + exacerbating cognitive deterioration, and when conjoined with T +, even swifter decline in cognitive function has been demonstrated [7]. These findings are congruent with our own results. In more recent investigations, A + T + has been shown to be associated with an accelerated accumulation of tau in the neocortical region compared with both A − T − and A + T − [10]. Given that the site of tau deposition serves as a predictive indicator for subsequent atrophy within the same cerebral region [45], it is reasonable to anticipate that the presence of A + T + would lead to substantial acceleration of tau deposition and atrophy across the entire cerebral domain. Ultimately, such a process could be poised to induce expedited global cognitive decline.

In contrast, the A − T + group did not show further brain atrophy or decline in cognitive function compared with the reference group, indicating that T + alone does not promote brain atrophy or cognitive decline. Similar to our results, previous studies have also shown that A − T + is not associated with accelerated cognitive decline compared with A − T − [10, 46, 47]. It has been reported that primary age-related tauopathy (PART) [48], a condition probably encompassed within A − T + [49], exhibits an absence of subsequent amyloid elevation, while tau aggregation remains confined to the temporal lobe [10]. Furthermore, the rate of tau accumulation and cognitive decline in PART appears to proceed at a more gradual pace than that observed in individuals with A + T + [10]. Our results support that the A − T + group does not follow the same progressive trajectory as the A + T + group with regard to brain atrophy and cognitive decline.

In the model that incorporated interactions between covariates and time as a sensitivity analysis, we observed significant associations between the baseline age and longitudinal changes in the expansion of the lateral ventricles and cortical thinning. The association between age and the rate of brain atrophy in these regions is supported by our findings and those of other studies [50–52]. Therefore, it is essential to account for the interaction between age and time when conducting longitudinal analyses of volume or cortical thickness in these areas. On the other hand, no significant associations were observed between sex or *APOE* genotype and the rate of brain atrophy. There are conflicting reports regarding the association between sex and brain atrophy rates [50, 52]. Although some studies have suggested an association between the *APOE* genotype and atrophy rates in the medial temporal regions [52, 53], our results are not in accordance with these findings. These conflicting findings highlight the need for further research to further elucidate this relationship.

Additional sub-analyses using a generalized linear mixed-effects model with linear and quadratic terms for time and their interaction with the group using data from the entire period showed similar results to those of the main analysis using only the linear term for time with respect to whole brain and lateral ventricle volumes and cortical thickness in the AD-signature regions. While the A + T − and A + T + groups showed greater acceleration of decline (quadratic effect) than the A − T − group in terms of the PACC scores, only the A + T − group showed greater acceleration of volume loss in the hippocampus. The reason why the A + T + group did not show a significantly greater hippocampal volume reduction with respect to the linear and/or quadratic terms of time than the A − T − group is unclear. However, one possibility is that the data after 7.5 years from baseline may have been affected by outliers due to few observations.

In this study, the structural MRI scans were longitudinally acquired from scanners from different sites, scanner manufacturers, and magnetic field strengths of 1.5 T and 3 T, which may have introduced undesirable, nonbiological technical variations in the inter- and/or intrasubject measurements obtained from them [54–56]. Image

Fujishima *et al. Alzheimer's Research & Therapy*   (2024) 16:77

Page 13 of 16

harmonization techniques, such as longitudinal ComBat, may minimize such non-biological sources of variances among different scanners in this multisite longitudinal study [37, 57]. Thus, we employed longitudinal ComBat (via longCombat package in R) to harmonize the MRI measurements, aiming to mitigate the non-biological variability for the sensitivity analyses. In the sub-analysis that included the quadratic term for time and interaction terms between group and the quadratic term for time across the four groups for the entire period, none of the groups demonstrated a significant reduction in longitudinal whole brain volume compared with the reference $A-T-$ group. This observation could potentially be explained by the regulation of Type 1 errors through longitudinal ComBat, as indicated by Beer et al. [37]. Nonetheless, other findings showed negligible discrepancies compared with the outcomes derived from the examination of data that had not been harmonized.

In our results of the survival analysis, only the $A+T+$ and $A+T-$ groups showed a statistically significant increased risk of progression to MCI or dementia compared with the reference $A-T-$ group. Prior studies have demonstrated that $A+T+$ is associated with a higher risk of disease progression in AD than $A-T-$ [6, 7], and our results are consistent with those findings. Populations with a combination of $A+$ and $T+$ are at higher risk for disease progression in AD during the preclinical stage; therefore, therapeutic intervention in these populations may effectively inhibit disease progression. The $A+T-$ group also demonstrated an increased risk of disease progression to MCI or dementia compared with the reference group. As mentioned earlier, it is plausible that among cases classified as $A+T-$, there were instances where the determination of tau pathology via CSF p-tau181 resulted in false negatives. This potential misclassification might have influenced the observed risk elevation within this group.

Treatments for MCI and mild dementia using anti-amyloid antibodies such as lecanemab and donanemab have been shown to slow down cognitive decline in Phase 3 clinical trials, but they have not demonstrated the ability to halt cognitive decline [1, 2]. Our study has shown that elderly individuals with preclinical AD classified as $A+T+$ experience accelerated brain atrophy and cognitive decline compared with those classified as $A-T-$. This suggests that proactive treatment in such elderly individuals with anti-amyloid antibodies, as in the AHEAD trial or TRAILBLAZER-ALZ3 (NCT05026866), or treatment targeting tau might help in preventing the progression of brain atrophy and cognitive decline. However, one meta-analysis indicated that certain anti-amyloid therapies including some anti-amyloid antibodies and secretase inhibitors may accelerate brain atrophy [58]. It remains unclear whether this atrophy is a result of these treatments exacerbating neurodegeneration or due to other causes; thus, further research is needed.

Limitations of the study

Our study has four limitations:

1) We had a small number of observations after 7.5 years. Therefore, analyses of brain morphology and cognitive function for the entire period including after 7.5 years may have been influenced by outliers. Survival analyses also may have been affected by selection bias due to dropouts after 7.5 years. It is anticipated that at least half of the ADNI3 participants will continue to participate in ADNI4 [59], which may make it possible to analyze observational data over a longer period of time.

2) In our analysis, we compared linear and quadratic models. Despite the better fit of the quadratic models as indicated by their lower AIC values, we selected a linear model due to its simplicity and clinical interpretability. This decision balanced model complexity with interpretability, which is crucial for clinical application. However, we acknowledge that quadratic models may capture data nuances more accurately; thus, further exploration in future studies is warranted.

3) We used CSF Aβ42 to evaluate $A+/-$ instead of the concentration ratio of Aβ42 to Aβ40 (Aβ42/40 ratio) because there were numerous cases in which Aβ40 was not measured in the ADNI data. The Aβ42/40 ratio is more accurate in diagnosing patients with AD than Aβ42 alone; therefore, Hansson et al. advocate using the former when analyzing CSF AD biomarkers [60]. Future studies should be able to discriminate $A+/-$ with higher accuracy using the Aβ42/40 ratio.

4) We used CSF p-tau181 to evaluate $T+/-$. While CSF p-tau181 is a biomarker for T that represents changes in tau metabolism in the AT(N) system [5], elevated CSF p-tau181 levels are more strongly associated with cerebral amyloidosis than with neurofibrillary tangles [61]. Due to the potential of CSF p-tau205 and CSF microtubule-binding region (MTBR) of tau containing the residue 243 (MTBR-tau243) as indicators of tau tangles [62], employing T defined by Tau-PET, CSF p-tau205, or CSF MTBR-tau243 would allow for a longitudinal study of cognitively healthy individuals in a condition that better reflects the pathological changes of amyloid plaques and neurofibrillary tangles.

Fujishima *et al. Alzheimer's Research & Therapy* (2024) 16:77

Page 14 of 16

Conclusions

Within the healthy elderly population, A+, when combined with T+, exacerbates cerebral atrophy in the regions related to AD, leading to accelerated disease progression. Notably, in isolation, T+ does not provoke cerebral atrophy, cognitive decline, or disease progression. The implementation of therapeutic intervention in cognitively normal individuals with A+T+ may serve as a pivotal strategy in forestalling subsequent cerebral atrophy, cognitive deterioration, and disease progression.

Abbreviations

Aβ42	Amyloid-beta 42
AD	Alzheimer's disease
ADNI	Alzheimer's Disease Neuroimaging Initiative
AIC	Akaike Information Criterion
APOE	Apolipoprotein E
A−	Amyloid negative
A+	Amyloid positive
CDR	Clinical Dementia Rating
CSF	Cerebrospinal fluid
DBC	Differential bias correction
DiReCT	Diffeomorphic registration-based cortical thickness
DL	Deep learning-based neuroanatomy segmentation and cortex parcellation
KN-BSI	K-means normalized boundary shift integral
LOESS	Locally estimated scatterplot smoothing
MCI	Mild cognitive impairment
MMSE	Mini-Mental State Examination
MRI	Magnetic resonance imaging
MTBR-tau243	Microtubule-binding region of tau containing the residue 243
PACC	Preclinical Alzheimer Cognitive Composite
PART	Primary age-related tauopathy
PET	Positron emission tomography
p-tau181	Phosphorylated tau 181
T−	Tau negative
T+	Tau positive
WMS-R	Wechsler Memory Scale-Revised

Supplementary Information

The online version contains supplementary material available at https://doi.org/10.1186/s13195-024-01450-7.

> **Supplementary Material 1.**
>
> **Supplementary Material 2.**

Authors' contributions

MF designed the study, conducted data processing, interpreted the data, and drafted and revised the manuscript. YK and TM conducted statistical analyses and wrote and revised the manuscript. HM revised the manuscript. All authors read and approved the final manuscript.

Availability of data and materials

The ADNI data is publicly available on its database for approved individuals (https://adni.loni.usc.edu/). The processed data in this study are not publicly available because of space limitations but are available from the corresponding author on reasonable request.

Declarations

Ethics approval and consent to participate

The study was conducted in accordance with the Declaration of Helsinki. The Institutional Review Boards approved all research activities at the participating study sites. Participants provided written informed consent.

Consent for publication

Not applicable.

Competing interests

The authors declare no competing interests.

Author details

[1]Department of Radiology, Kumagaya General Hospital, 4-5-1 Nakanishi, Kumagaya 360-8567, Japan. [2]Department of Biostatistics, Graduate School of Medicine, Saitama Medical University, 38 Morohongo, Moroyama 350-0495, Japan. [3]Biostatistics Section, Clinical Research Center, Chiba University Hospital, 1-8-1 Inohana, Chuo-Ku, Chiba 260-8670, Japan. [4]Center for Innovative Clinical Medicine, Okayama University Hospital, 2-5-1 Shikata-Cho, Kita-Ku, Okayama 700-8558, Japan. [5]Department of Biofunctional Imaging, Fukushima Medical University, 1 Hikariga-Oka, Fukushima 960-1295, Japan. [6]Drug Discovery and Cyclotron Research Center, Southern Tohoku Research Institute for Neuroscience, 7-61-2 Yatsuyamada, Koriyama 963-8052, Japan.

References

1. van Dyck CH, Swanson CJ, Aisen P, Bateman RJ, Chen C, Gee M, et al. Lecanemab in early Alzheimer's disease. N Engl J Med. 2023;388:9–21.
2. Sims JR, Zimmer JA, Evans CD, Lu M, Ardayfio P, Sparks J, et al. Donanemab in early symptomatic Alzheimer disease: the TRAILBLAZER-ALZ 2 randomized clinical trial. JAMA. 2023;330:512–27.

3. Selkoe DJ, Hardy J. The amyloid hypothesis of Alzheimer's disease at 25 years. EMBO Mol Med. 2016;8:595–608.

4. Rafii MS, Sperling RA, Donohue MC, Zhou J, Roberts C, Irizarry MC, et al. The AHEAD 3–45 Study: Design of a prevention trial for Alzheimer's disease. Alzheimers Dement. 2023;19:1227–33.

5. Jack CR, Bennett DA, Blennow K, Carrillo MC, Dunn B, Haeberlein SB, et al. NIA-AA research framework: toward a biological definition of Alzheimer's disease. Alzheimers Dement. 2018;14:535–62.

6. Strikwerda-Brown C, Hobbs DA, Gonneaud J, St-Onge F, Binette AP, Ozlen H, et al. Association of elevated amyloid and tau positron emission tomography signal with near-term development of Alzheimer disease symptoms in older adults without cognitive impairment. JAMA Neurol. 2022;79:975.

7. Ossenkoppele R, Pichet Binette A, Groot C, Smith R, Strandberg O, Palmqvist S, et al. Amyloid and tau PET-positive cognitively unimpaired individuals are at high risk for future cognitive decline. Nat Med. 2022;28:2381–7.

8. Desikan RS, McEvoy LK, Thompson WK, Holland D, Roddey JC, Blennow K, et al. Amyloid-β associated volume loss occurs only in the presence of phospho-tau. Ann Neurol. 2011;70:657–61.

9. Xie L, Wisse LEM, Das SR, Vergnet N, Dong M, Ittyerah R, et al. Longitudinal atrophy in early Braak regions in preclinical Alzheimer's disease. Hum Brain Mapp. 2020;41:4704–17.

10. Costoya-Sánchez A, Moscoso A, Silva-Rodríguez J, Pontecorvo MJ, Devous MD, Aguiar P, et al. Increased medial temporal tau positron emission tomography uptake in the absence of amyloid-β positivity. JAMA Neurol. 2023.

11. Dubois B, Hampel H, Feldman HH, Scheltens P, Aisen P, Andrieu S, et al. Preclinical Alzheimer's disease: definition, natural history, and diagnostic criteria. Alzheimers Dement. 2016;12:292–323.

12. Folstein MF, Folstein SE, McHugh PR. Mini-mental state. J Psychiatr Res. 1975;12:189–98.

13. Morris JC. The Clinical Dementia Rating (CDR): current version and scoring rules. Neurology. 1993;43:2412.2-2412-a.

14. Wechsler D. Wechsler memory scale-revised. New York: Psychological Corporation; 1987.

15. Bittner T, Zetterberg H, Teunissen CE, Ostlund RE, Militello M, Andreasson U, et al. Technical performance of a novel, fully automated electrochemiluminescence immunoassay for the quantitation of β-amyloid (1–42) in human cerebrospinal fluid. Alzheimers Dement. 2016;12:517–26.

16. Hansson O, Seibyl J, Stomrud E, Zetterberg H, Trojanowski JQ, Bittner T, et al. CSF biomarkers of Alzheimer's disease concord with amyloid-β PET and predict clinical progression: a study of fully automated immunoassays in BioFINDER and ADNI cohorts. Alzheimers Dement. 2018;14:1470–81.

17. Dumurgier J, Sabia S, Zetterberg H, Teunissen CE, Hanseeuw B, Orellana A, et al. A pragmatic, data-driven method to determine cutoffs for CSF biomarkers of Alzheimer disease based on validation against PET imaging. Neurology. 2022;99:e669–78.

18. Jack CR, Bernstein MA, Fox NC, Thompson P, Alexander G, Harvey D, et al. The Alzheimer's disease neuroimaging initiative (ADNI): MRI methods. J Magn Reson Imaging. 2008;27:685–91.

19. Tustison NJ, Avants BB, Cook PA, Yuanjie Z, Egan A, Yushkevich PA, et al. N4ITK: improved N3 bias correction. IEEE Trans Med Imaging. 2010;29:1310–20.

20. Manjón JV, Coupé P, Martí-Bonmatí L, Collins DL, Robles M. Adaptive non-local means denoising of MR images with spatially varying noise levels: spatially adaptive nonlocal denoising. J Magn Reson Imaging. 2010;31:192–203.

21. Modat M, Cash DM, Daga P, Winston GP, Duncan JS, Ourselin S. Global image registration using a symmetric block-matching approach. J Med Imaging (Bellingham). 2014;1:024003.

22. Ourselin S, Roche A, Subsol G, Pennec X, Ayache N. Reconstructing a 3D structure from serial histological sections. Image Vis Comput. 2001;19:25–31.

23. Avants BB, Yushkevich P, Pluta J, Minkoff D, Korczykowski M, Detre J, et al. The optimal template effect in hippocampus studies of diseased populations. Neuroimage. 2010;49:2457–66.

24. Avants BB, Tustison NJ, Song G, Cook PA, Klein A, Gee JC. A reproducible evaluation of ANTs similarity metric performance in brain image registration. Neuroimage. 2011;54:2033–44.

25. Rebsamen M, Rummel C, Reyes M, Wiest R, McKinley R. Direct cortical thickness estimation using deep learning-based anatomy segmentation and cortex parcellation. Hum Brain Mapp. 2020;41:4804–14.

26. Das SR, Avants BB, Grossman M, Gee JC. Registration based cortical thickness measurement. Neuroimage. 2009;45:867–79.

27. Desikan RS, Ségonne F, Fischl B, Quinn BT, Dickerson BC, Blacker D, et al. An automated labeling system for subdividing the human cerebral cortex on MRI scans into gyral based regions of interest. Neuroimage. 2006;31:968–80.

28. Jack CR, Wiste HJ, Weigand SD, Therneau TM, Lowe VJ, Knopman DS, et al. Defining imaging biomarker cut points for brain aging and Alzheimer's disease. Alzheimers Dement. 2017;13:205–16.

29. Leung KK, Clarkson MJ, Bartlett JW, Clegg S, Jack CR, Weiner MW, et al. Robust atrophy rate measurement in Alzheimer's disease using multi-site serial MRI: Tissue-specific intensity normalization and parameter selection. Neuroimage. 2010;50:516–23.

30. Thyreau B, Sato K, Fukuda H, Taki Y. Segmentation of the hippocampus by transferring algorithmic knowledge for large cohort processing. Med Image Anal. 2018;43:214–28.

31. Leung KK, Ridgway GR, Ourselin S, Fox NC. Consistent multi-time-point brain atrophy estimation from the boundary shift integral. Neuroimage. 2012;59:3995–4005.

32. Lewis EB, Fox NC. Correction of differential intensity inhomogeneity in longitudinal MR images. Neuroimage. 2004;23:75–83.

33. Hobbs NZ, Henley SMD, Wild EJ, Leung KK, Frost C, Barker RA, et al. Automated quantification of caudate atrophy by local registration of serial MRI: Evaluation and application in Huntington's disease. Neuroimage. 2009;47:1659–65.

34. Donohue MC, Sperling RA, Petersen R, Sun C-K, Weiner MW, Aisen PS, et al. Association between elevated brain amyloid and subsequent cognitive decline among cognitively normal persons. JAMA. 2017;317:2305–16.

35. Cleveland WS, Grosse E, Shyu WM. Local regression models. Statistical models in S. Wadsworth & Brooks/Cole; 1992. p. 309–76.

36. Akaike H. A new look at the statistical model identification. IEEE Trans Automat Contr. 1974;19:716–23.

37. Beer JC, Tustison NJ, Cook PA, Davatzikos C, Sheline YI, Shinohara RT, et al. Longitudinal ComBat: a method for harmonizing longitudinal multi-scanner imaging data. Neuroimage. 2020;220:117129.

38. Bernal-Rusiel JL, Greve DN, Reuter M, Fischl B, Sabuncu MR, Alzheimer's Disease Neuroimaging Initiative. Statistical analysis of longitudinal neuroimage data with Linear Mixed Effects models. Neuroimage. 2013;66:249–60.

39. Thomas KR, Bangen KJ, Weigand AJ, Edmonds EC, Wong CG, Cooper S, et al. Objective subtle cognitive difficulties predict future amyloid accumulation and neurodegeneration. Neurology. 2020;94:e397-406.

40. Ye BS, Lee Y, Kwak K, Park Y-H, Ham JH, Lee JJ, et al. Posterior ventricular enlargement to differentiate dementia with lewy bodies from Alzheimer's disease. J Alzheimers Dis. 2016;52:1237–43.

41. Khadhraoui E, Müller SJ, Hansen N, Riedel CH, Langer P, Timäeus C, et al. Manual and automated analysis of atrophy patterns in dementia with Lewy bodies on MRI. BMC Neurol. 2022;22:114.

42. Jochems ACC, Muñoz Maniega S, Del C Valdés Hernández M, Barclay G, Anblagan D, Ballerini L, et al. Contribution of white matter hyperintensities to ventricular enlargement in older adults. NeuroImage: Clinical. 2022;34:103019.

43. Vromen EM, De Boer SCM, Teunissen CE, Rozemuller A, Sieben A, Bjerke M, et al. Biomarker A+T−: is this Alzheimer's disease or not? A combined CSF and pathology study. Brain. 2023;146:1166–74.

44. Chou Y-Y, Leporé N, Saharan P, Madsen SK, Hua X, Jack CR, et al. Ventricular maps in 804 ADNI subjects: correlations with CSF biomarkers and clinical decline. Neurobiol Aging. 2010;31:1386–400.

45. La Joie R, Visani AV, Baker SL, Brown JA, Bourakova V, Cha J, et al. Prospective longitudinal atrophy in Alzheimer's disease correlates with the intensity and topography of baseline tau-PET. Sci Transl Med. 2020;12:eaau5732.

46. Soldan A, Pettigrew C, Fagan AM, Schindler SE, Moghekar A, Fowler C, et al. ATN profiles among cognitively normal individuals and longitudinal cognitive outcomes. Neurology. 2019;92:e1567–79.

47. Erickson P, Simrén J, Brum WS, Ennis GE, Kollmorgen G, Suridjan I, et al. Prevalence and clinical implications of a β-Amyloid–negative,

tau-positive cerebrospinal fluid biomarker profile in Alzheimer disease. JAMA Neurol. 2023

48. Crary JF, Trojanowski JQ, Schneider JA, Abisambra JF, Abner EL, Alafuzoff I, et al. Primary age-related tauopathy (PART): a common pathology associated with human aging. Acta Neuropathol. 2014;128:755–66.

49. Jack CR, Wiste HJ, Weigand SD, Therneau TM, Knopman DS, Lowe V, et al. Age-specific and sex-specific prevalence of cerebral β-amyloidosis, tauopathy, and neurodegeneration in cognitively unimpaired individuals aged 50–95 years: a cross-sectional study. Lancet Neurol. 2017;16:435–44.

50. Takao H, Hayashi N, Ohtomo K. A longitudinal study of brain volume changes in normal aging. Eur J Radiol. 2012;81:2801–4.

51. Hua X, Hibar DP, Lee S, Toga AW, Jack CR, Weiner MW, et al. Sex and age differences in atrophic rates: an ADNI study with n=1368 MRI scans. Neurobiol Aging. 2010;31:1463–80.

52. Holland D, Desikan RS, Dale AM, McEvoy LK. Higher rates of decline for women and *Apolipoprotein E* ε4 carriers. AJNR Am J Neuroradiol. 2013;34:2287–93.

53. Donix M, Burggren AC, Suthana NA, Siddarth P, Ekstrom AD, Krupa AK, et al. Longitudinal changes in medial temporal cortical thickness in normal subjects with the APOE-4 polymorphism. Neuroimage. 2010;53:37–43.

54. Han X, Jovicich J, Salat D, Van Der Kouwe A, Quinn B, Czanner S, et al. Reliability of MRI-derived measurements of human cerebral cortical thickness: The effects of field strength, scanner upgrade and manufacturer. Neuroimage. 2006;32:180–94.

55. Jovicich J, Czanner S, Greve D, Haley E, Van Der Kouwe A, Gollub R, et al. Reliability in multi-site structural MRI studies: Effects of gradient non-linearity correction on phantom and human data. Neuroimage. 2006;30:436–43.

56. Takao H, Hayashi N, Ohtomo K. Effect of scanner in longitudinal studies of brain volume changes. J Magn Reson Imaging. 2011;34:438–44.

57. Fortin J-P, Cullen N, Sheline YI, Taylor WD, Aselcioglu I, Cook PA, et al. Harmonization of cortical thickness measurements across scanners and sites. Neuroimage. 2018;167:104–20.

58. Alves F, Kalinowski P, Ayton S. Accelerated brain volume loss caused by anti–β-Amyloid drugs: a systematic review and meta-analysis. Neurology. 2023;100:e2114–24.

59. Weiner MW, Veitch DP, Miller MJ, Aisen PS, Albala B, Beckett LA, et al. Increasing participant diversity in AD research: Plans for digital screening, blood testing, and a community-engaged approach in the Alzheimer's disease neuroimaging initiative 4. Alzheimers Dement. 2023;19:307–17.

60. Hansson O, Lehmann S, Otto M, Zetterberg H, Lewczuk P. Advantages and disadvantages of the use of the CSF Amyloid β (Aβ) 42/40 ratio in the diagnosis of Alzheimer's disease. Alzheimers Res Ther. 2019;11:34.

61. Barthélemy NR, Li Y, Joseph-Mathurin N, Gordon BA, Hassenstab J, Benzinger TLS, et al. A soluble phosphorylated tau signature links tau, amyloid and the evolution of stages of dominantly inherited Alzheimer's disease. Nat Med. 2020;26:398–407.

62. Horie K, Salvadó G, Barthélemy NR, Janelidze S, Li Y, He Y, et al. CSF MTBR-tau243 is a specific biomarker of tau tangle pathology in Alzheimer's disease. Nat Med. 2023;29:1954–63.

Publisher's Note